New Developments in High Temperature Processing of Steels and Related Materials Leading the Sustainable Society, and Key Properties of High Temperature Melts

ISIJ International, Vol. 64 (2024), No. 15, pp. 2245–2252
https://doi.org/10.2355/isijinternational.ISIJINT-2024-141

# Phonon Mean Free Path of Silicate Glasses: A Useful Parameter to Distinguish between Framework and Nonframework Cations

Sohei SUKENAGA,[1)*] Bunta OZATO,[2)] Yohei ONODERA,[3)] Shinji KOHARA,[3)] Masahiro SHIMIZU,[4)] Tsuyoshi NISHI,[5)] Rie ENDO,[6)] Takaaki TOMAI,[1,7)] Akira YOKO,[8,9)] Sakiko KAWANISHI,[10)] Hiroshi FUKAYA,[11)] Hiromichi OHTA[5)] and Hiroyuki SHIBATA[1)]

1) Institute of Multidisciplinary Research for Advanced Materials, Tohoku University, 2-1-1 Katahira, Aoba-ku, Sendai, 9808577 Japan.
2) Department of Metallurgy, Graduate School of Engineering, Tohoku University, 6-6 Aramaki Aza Aoba, Aoba-ku, Sendai, 9808579 Japan.
3) Center for Basic Research on Materials, National Institute for Materials Science, 1-2-1 Sengen, Tsukuba, Ibaraki, 3050047 Japan.
4) Department of Material Chemistry, Graduate School of Engineering, Kyoto University, Katsura, Nishikyo-ku, Kyoto, 6158510 Japan.
5) Department of Materials Science and Engineering, Graduate School of Science and Engineering, Ibaraki University, Hitachi, Ibaraki, 3168511 Japan.
6) College of Engineering, Shibaura Institute of Technology, Koto-ku, Tokyo, 1358548 Japan.
7) Frontier Research Institute for Interdisciplinary Sciences, Tohoku University, 6-3 Aramaki Aza Aoba, Aoba-ku, Sendai, 9808578 Japan.
8) WPI-Advanced Institute for Materials Research (WPI-AIMR), Tohoku University, 2-1-1 Katahira, Aoba-ku, Sendai, 9808577 Japan.
9) International Center for Synchrotron Radiation Innovation Smart, Tohoku University, 468-1 Aramaki Aza Aoba, Aoba-ku, Sendai, 9808572 Japan.
10) Department of Energy Science and Technology, Graduate School of Energy Science, Kyoto University, Yoshida-honmachi, Sakyo-ku, Kyoto, 6068501 Japan.
11) Graduate School of Engineering, Tohoku University, 6-6 Aramaki Aza Aoba, Aoba-ku, Sendai, 9808579 Japan.

(*Received April 30, 2024; Accepted August 29, 2024; Advance online published September 11, 2024; Published December 30, 2024*)

Assuming that heat is transported by lattice vibrations (phonons) in silicate glasses, their thermal conductivity is correlated with the product of sound velocity, volumetric heat capacity, and phonon mean free path (MFP). The sound velocity and heat capacity have been studied extensively, but the origin of the composition-induced variation in the MFP remains unclear. The present study investigated MFP in $M_{2/n}O$–$SiO_2$ ($M^{n+}$: $Li^+$, $Na^+$, $Ca^{2+}$, $Sr^{2+}$, or $Pb^{2+}$) glasses with a variation of $M_{2/n}O$ content. The MFP of the silica glass decreased with the addition of $M_{2/n}O$. The effect of the type of metallic cation on the MFP was minimal for the selected alkali and alkaline-earth silicate glasses. By contrast, the MFP of lead silicate glasses was higher than those of alkali or alkaline-earth silicate glasses when the metallic cation contents were comparable. Previous studies have demonstrated that alkali and alkaline-earth cations act as nonframework species that break the silicate network structure, whereas lead cations have inconclusive structural roles. Our data indicate that lead cations partly act as framework cations and that phonons tend to be scattered near nonframework cations in silicate glasses. Thus, the phonon MFP is a useful parameter for determining the structural role of metallic cations in silicate glass via phonon propagation.

KEY WORDS: phonon mean free path; silicate glasses and melts; sound velocity; thermal conductivity; framework and non-framework cations.

## 1. Introduction

Understanding the thermophysical properties of the metal and oxide phases is essential for designing heat transfer in high-temperature industries (*e.g.*, metallurgical extraction[1,2] and glass-making[3]), directly affecting the efficiency and accuracy of these processes. For example, in the continuous casting process of steel, it is essential to control the rate of

* Corresponding author: E-mail: sohei.sukenaga.d3@tohoku.ac.jp

heat removal from cast steel to suppress the formation of defects on its surface.[4,5] The mold flux is used as a thermal insulator between the mold and cast steel and plays an important role in controlling the rate of heat removal.[4,6,7] In general, mold flux is composed of at least three phases: silicate glass, crystals, and melt.[8–10] Understanding the various thermophysical properties (*e.g.*, thermal conductivity) that dominate the conduction and radiation heat transfer through a multiphase thermal insulator (*i.e.*, mold flux) is important for controlling the rate of heat removal. The dominant factors that control the thermophysical properties of crystalline phases have been studied by numerous researchers;[11,12] however, the mechanism of composition-induced variation in the thermal conductivity of silicate melts and glasses is poorly understood.[13] Hence, it is difficult to design flux compositions with optimal thermal conductivity. Assuming that the heat carrier in these noncrystalline phases is mainly a lattice vibration wave, *i.e.*, phonon,[14,15] the thermal conductivity ($\lambda$ [W m$^{-1}$ s$^{-1}$]) can be expressed as a function of the volumetric heat capacity ($C_V$ [J m$^{-3}$ K$^{-1}$]), velocity of sound ($v$ [m s$^{-1}$]), and mean free path (MFP) of phonons ($l$ [m]), as expressed in Eq. (1):[16]

$$\lambda = \frac{1}{3} C_V v l, \quad \text{..... (1)}$$

An in-depth discussion of these three parameters can provide a complete understanding of the thermal conductivities of noncrystalline materials. The compositional dependence of the $C_V$ and $v$ of silicate glasses and melts has been studied well in the previous studies,[17–20] whereas the MFP of phonon is one of the least understood parameters. Previous studies have reported two important findings related to phonon MFP in silicate glasses and melts:

- The MFP of phonon is generally in the range of 0.3–0.7 nm.[21–23]
- The phonon MFP decreases with the addition of metallic oxides (*e.g.*, $Na_2O$).[15,24–26]

The former indicates that the phonon MFP should reflect the structure on the length scale between a silicon atom and its second-neighbor cation ($Si^{4+}$ or $M^{n+}$),[27] which is schematically illustrated in **Fig. 1** for the case of the structure between silicon and the second-neighbor silicon cation ($Si–Si_{2nd}$). The latter indicates that the incoherent vibrations near the metallic cations tend to scatter phonons and reduce the MFP. However, it remains unclear whether the phonon MFP depends on the type and content of metallic cations in silicate glasses. In addition, the origin of phonon scattering near metallic cations remains unclear. As our previous study indicated that the compositional dependence of the phonon MFP in silicate glasses is similar to that of these melts,[15] glasses can be used as analog materials to understand the compositional dependence of the phonon MFP in their melts. The present study aimed to investigate the compositional dependence of the phonon MFP for selected binary silicate glasses containing several types of metallic oxides, which are important for mold fluxes, metallurgical slags, and glass materials, as a fundamental study of the metallic cation-induced phonon scattering behavior in silicate glasses and melts.

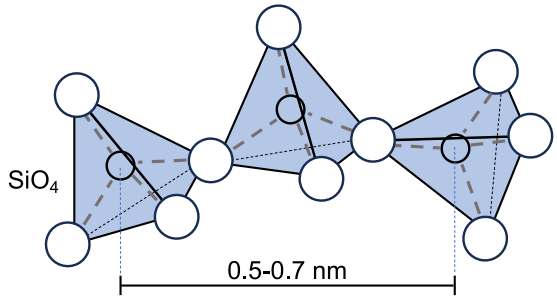


**Fig. 1.** Schematic illustrations of the linkage of $SiO_4$ tetrahedra with its length scale. A typical range of $Si–Si_{2nd}$ interatomic distance is described according to a reported value.[27] (Online version in color.)

## 2. Principle to Derive the Phonon MFP

The thermal conductivity ($\lambda$) of the glass samples is correlated with the thermal diffusivity ($\alpha$ [m$^2$ s$^{-1}$]) by the following Eq. (2):[28]

$$\lambda = \alpha \rho C_P, \quad \text{..... (2)}$$

where $\rho$ [kg m$^{-3}$] is the density and $C_P$ [J kg$^{-1}$ K$^{-1}$] is the specific heat capacity. From Eqs. (1) and (2), the MFP of phonon ($l$) be expressed by Eq. (3) where $C_V = \rho C_P$:

$$l = \frac{3\alpha}{v}. \quad \text{..... (3)}$$

The present study has measured the thermal diffusivity ($\alpha$) and velocity of sound ($v$) for the glass samples to determine the phonon MFP ($l$).

## 3. Experimental Method

### 3.1. Sample Synthesis

The nominal and analyzed compositions of the glass samples are listed in **Table 1**. Glass samples with the composition of $x$ mol% $M_{2/n}O$–(100-$x$) mol% $SiO_2$ (M: Li, Na, Ca, Sr, or Pb) were labeled as MS$x$ where n represents the valence number of the metallic cation. The glasses were fabricated using melting and quenching methods. Reagent powders of $SiO_2$ (FUJIFILM Wako Pure Chemical Corporation), $Li_2CO_3$ (Sigma-Aldrich Co. LLC), $Na_2CO_3$ (Sigma-Aldrich Co. LLC), $CaCO_3$ (FUJIFILM Wako Pure Chemical Corporation), and $SrCO_3$ (Sigma-Aldrich Co. LLC) were mixed using a mullite mortar and pestle to obtain starting powder mixtures for the alkali or alkaline earth silicate glasses. To avoid the precipitation of metallic Pb,[29] powder mixtures of PbO (FUJIFILM Wako Pure Chemical Corporation), $Pb(NO_3)_2$ (FUJIFILM Wako Pure Chemical Corporation), and $SiO_2$ (FUJIFILM Wako Pure Chemical Corporation) were prepared to synthesize lead silicate glasses. The powder mixtures were placed in a Pt–5mass%Au crucible (silica crucible for lead silicate glass) and calcined at 1 073–1 273 K for 30 min. The obtained samples were melted at 1 273–1 873 K in a Pt–5mass%Au crucible, which is less wettable to silicate melts.[30] Finally, the molten sample was cast into a graphite mold. The quenched glass was annealed at a temperature close to the glass transition temperature.[31,32] Annealed samples were used for the property measurements. Because it was difficult to melt pure silica (*i.e.*, $SiO_2$) in the laboratory, a standard

**Table 1.** Nominal and analyzed compositions of the samples in mol%. The analyzed compositions are shown in parentheses. $f_{Si-O-M}$ values were calculated using Eq. (7) with the analyzed compositions.

| Samples | $SiO_2$ | $Li_2O$ | $Na_2O$ | CaO | SrO | PbO | $f_{Si-O-M}$ |
|---|---|---|---|---|---|---|---|
| S | 100 | – | – | – | – | – | 0 |
| LiS28 | 72.0 | 28.0 | – | – | – | – | |
| | (71.3) | (28.7) | – | – | – | – | (0.34) |
| LiS33 | 67.0 | 33.0 | – | – | – | – | |
| | (66.8) | (33.2) | – | – | – | – | (0.40) |
| LiS36 | 64.0 | 36.0 | – | – | – | – | |
| | (64.0) | (36.0) | – | – | – | – | (0.44) |
| NaS18 | 82.0 | – | 18.0 | – | – | – | |
| | (81.5) | – | (18.5) | – | – | – | (0.20) |
| NaS23 | 77.0 | – | 23.0 | – | – | – | |
| | (77.6) | – | (22.4) | – | – | – | (0.25) |
| NaS28 | 72.0 | – | 28.0 | – | – | – | |
| | (72.2) | – | (27.8) | – | – | – | (0.32) |
| NaS33 | 67.0 | – | 33.0 | – | – | – | |
| | (67.5) | – | (32.5) | – | – | – | (0.39) |
| NaS36 | 64.0 | – | 36.0 | – | – | – | |
| | (64.5) | – | (35.5) | – | – | – | (0.43) |
| CaS42 | 58.0 | – | – | 42.0 | – | – | |
| | (59.2) | – | – | (40.8) | – | – | (0.51) |
| CaS45 | 55.0 | – | – | 45.0 | – | – | |
| | (55.4) | – | – | (44.6) | – | – | (0.57) |
| SrS40 | 60.0 | – | – | – | 40.0 | – | |
| | (63.4) | – | – | – | (36.6) | – | (0.45) |
| PbS33 | 67.0 | – | – | – | – | 33.0 | |
| | (66.7) | – | – | – | – | (33.3) | (0.40) |
| PbS50 | 50.0 | – | – | – | – | 50.0 | |
| | (48.0) | – | – | – | – | (52.0) | (0.70) |
| PbS60 | 40.0 | – | – | – | – | 60.0 | |
| | (43.1) | – | – | – | – | (56.9) | (0.80) |

quartz glass (5809-a, National Institute of Advanced Industrial Science and Technology)[33] was used for the thermal diffusivity measurements. In addition, the chemical compositions of the synthesized samples were tested using wet chemical analyses; the lithium, sodium, calcium, strontium, and lead contents of the samples were measured using inductively coupled plasma atomic emission spectrometry (ICP-AES), whereas the silicon content was determined by gravimetry.

### 3.2. Measurements of Thermal Diffusivity and Sound Velocity

The thermal diffusivity ($\alpha$) of the samples were evaluated using a flash method with a xenon flash lamp, which heats the front surface of the samples by a short energy pulse, and the resulting temperature response of the rear surface is measured with an infrared detector. The present study used a Xenon flash analyzer LFA 467 HyperFlash (NETZSCH, Japan) to determine the $\alpha$ of the samples. The synthesized glass samples were cylindrical (diameter: 10 mm; height: 1 mm). Because the synthesized glass samples were transparent, it was necessary to avoid the penetration of light generated by the xenon lamp. In addition, the flash method requires the surface of the samples to absorb the energy pulse and exhibit high emissivity.[34] The top and bottom surfaces of the samples were mirror polished and spray-coated with carbon powder (FC-153) after gold sputtering (~100 nm). The temperature response of the rear sample surface was measured thrice at 298 K for each sample. To determine the thermal diffusivity of the samples, the present study applied the Cape–Lehman model,[35] which considers the facial and radial heat losses in the temperature evolution of the rear sample surface over time after a short energy pulse. The model accurately reproduced the temperature evolution observed in this study. The repetitive errors in the three-time measurements were approximately 1% for most of the samples (see detail in **Table 2**).

The sound velocity ($v$ [m $s^{-1}$]) of the glass samples is defined by the following Eq. (4):[36]

$$v = \sqrt{\frac{E}{2\rho}}, \quad \text{..... (4)}$$

where $E$ is the Young's modulus of the samples, and $\rho$ is the sample density [kg $m^{-3}$]. Moreover, $E$ can be determined by the longitudinal ($v_L$) and transverse wave velocities ($v_T$) by the Eq. (5):[37]

$$E = \rho v_T^2 \frac{3v_L^2 - 4v_T^2}{v_L^2 - v_T^2}. \quad \text{..... (5)}$$

The present study measured the $v_L$ and $v_T$ of the samples using an ultrasonic wave propagation pulse-echo technique with a thickness gauge 38DL PLUS (OLYMPUS corporation, Japan). The glass was cylindrical (diameter: 10 mm, height: 10 mm), and the top and bottom surfaces were mirror-polished. The polished samples were used for measurements. The measurements were performed thrice at a frequency of 5 MHz for each sample at 298 K. The scatter in the measurements was less than 0.5%. The averaged values of $v_L$ and $v_T$ were used to derive the sound velocity of the samples. It is clear that Eqs. (4) and (5) enable us to derive sound velocity ($v$) without using the sample density ($\rho$); however, the $\rho$ of the sample is required to interpret the compositional dependence of $v$. The present study evaluated the $\rho$ of the samples using a conventional Archimedean method at ~298 K with ethanol (FUJIFILM Wako Pure Chemical Corporation) as the immersion liquid. The density of the samples was measured five times, and the average values were used to determine the sound velocities of the samples. The repetitive error in the measurements was less than 1.2%.

## 4. Results

### 4.1. Thermal Diffusivity

**Figure 2** and Table 2 show the composition-induced variations in the thermal diffusivities of the glass samples at 298 K. The measured thermal diffusivity of the pure silica glass ($0.829\times10^{-6}$ $m^2$ $s^{-1}$) is close to the recommended value

**Table 2.** Measured thermophysical properties of the samples at 298 K.

| Samples | $\alpha/10^{-6}$ m$^2$ s$^{-1}$ | $\rho/10^3$ kg m$^{-3}$ | $n_{Si-O-M}$/nm$^{-3}$ | $v_L$/m s$^{-1}$ | $v_T$/m s$^{-1}$ | $v$/m s$^{-1}$ | $E^{\#}$/GPa | $l$/nm |
|---|---|---|---|---|---|---|---|---|
| S | 0.824±0.005 | 2.187 | 0 | – | – | 4 288* | 80 | 0.58 |
| LiS28 | 0.574±0.002 | 2.328 | 5.22 | 6 160 | 3 710 | 4 090 | 78 | 0.42 |
| LiS33 | 0.555±0.071 | 2.333 | 6.21 | 6 283 | 3 658 | 4 079 | 78 | 0.41 |
| LiS36 | 0.531±0.004 | 2.349 | 6.90 | 6 372 | 3 701 | 4 130 | 80 | 0.39 |
| NaSI8 | 0.563±0.008 | 2.369 | 2.91 | 5 404 | 3 228 | 3 569 | 60 | 0.47 |
| NaS23 | 0.515±0.001 | 2.406 | 3.58 | 5 386 | 3 157 | 3 513 | 59 | 0.44 |
| NaS28 | 0.481±0.009 | 2.457 | 4.53 | 5 352 | 3 070 | 3 439 | 58 | 0.42 |
| NaS33 | 0.439±0.007 | 2.478 | 5.33 | 5 410 | 3 050 | 3 433 | 58 | 0.38 |
| NaS36 | 0.419±0.002 | 2.499 | 5.86 | 5 381 | 3 007 | 3 393 | 58 | 0.37 |
| CaS42 | 0.500±0.032 | 2.795 | 9.07 | 6 298 | 3 481 | 3 938 | 87 | 0.38 |
| CaS45 | 0.485±0.001 | 2.839 | 10.2 | 6 325 | 3 494 | 3 954 | 89 | 0.37 |
| SrS40 | 0.386±0.005 | 3.446 | 7.59 | 5 366 | 2 965 | 3 355 | 78 | 0.35 |
| PbS33 | 0.393±0.003 | 4.617 | 6.07 | 3 720 | 2 204 | 2 444 | 55 | 0.48 |
| PbS50 | 0.270±0.002 | 6.339 | 11.1 | 3 109 | 1 732 | 1 956 | 49 | 0.41 |
| PbS60 | 0.256±0.001 | 6.492 | 12.0 | 3 030 | 1 682 | 1 901 | 47 | 0.40 |

* Value reported by Manghnani and Singh[31]
$^{\#}$ $E$ values calculated using Eq. (4)

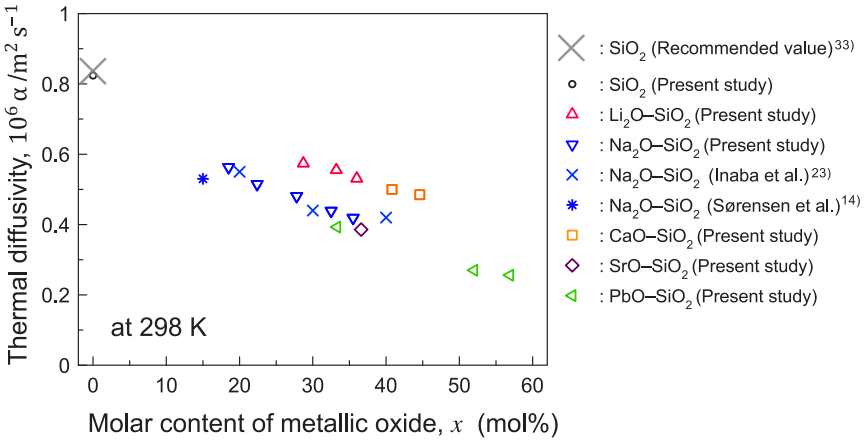


**Fig. 2.** The change in thermal diffusivity of the silicate glasses by adding metallic oxides. The horizontal axis shows the analyzed content of metallic oxides. (Online version in color.)

$(0.837\times10^{-6}$ m$^2$ s$^{-1})$.[33] This validates the reasonability of our methodology for determining the thermal diffusivity. The thermal diffusivity of the silica glass decreased with the addition of $Na_2O$. This trend agrees well with previous studies that reported the thermal diffusivity of $Na_2O$–$SiO_2$ glasses using the laser flash method.[14,15,23] Similarly, the thermal diffusivity of silica glass decreased with the addition of all types of chosen metallic oxides.

### 4.2. Velocity of Sound

**Figure 3** shows the effect of adding metallic oxide on the sound velocity in the sample glasses. Manghnani and Singh[31] measured the sound velocities of silica and sodium silicate glasses with compositions similar to those used in our study. Figure 3 compares their data with our results for the $Na_2O$–$SiO_2$ system. The differences between their values and our data for similar compositions were in the range of 3%–5%, which is sufficiently small to compare. Because preparing the sample with a pure silica composition for sound velocity measurement was difficult, a reported value for the silica composition by Manghnani and Singh is plotted in this figure. It was found that the sound velocity of silica glass did not significantly change with the addition of $Li_2O$ or CaO, whereas $Na_2O$ or PbO lowered the sound velocity. As shown in Eq. (4), the velocity of the sound is related to the ratio of Young's modulus to the density $(\sqrt{E/2\rho})$. Therefore, the glasses with low density and high Young's modulus (*e.g.*, $Li_2O$–$SiO_2$) have a higher sound velocity among the glasses chosen in the present study, whereas the low sound velocity of PbO–$SiO_2$ systems is likely due to their high density (see Table 2).

### 4.3. Phonon Mean Free Path (MFP)

In the kinetic theory of a gas, the MFP is generally defined as an average distance that a particle will move before a collision with another particle and is correlated

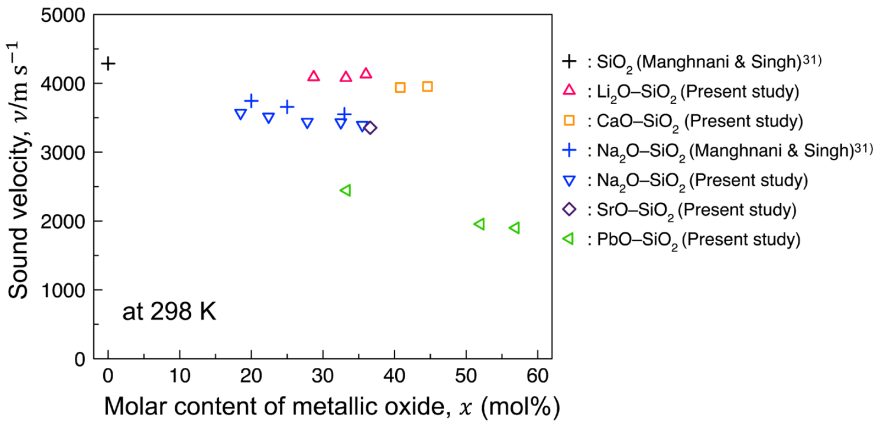


**Fig. 3.** Relationship between the sound velocity and the analyzed content of metallic oxides in the silicate glasses. (Online version in color.)

with the reciprocal number density of the particle per unit volume ($1/n_p$).[38] Applying this kinetic theory to the phonon propagation, the MFP of phonon can be considered as a distance of phonon propagation without scattering. Assuming that the phonons scattered near metallic cations, the phonon MFP should vary as a function of the number density of the oxygen atoms bonded with silicon and metallic cations ($n_{Si–O–M}$). The $n_{Si–O–M}$ [nm$^{-3}$] can be derived using the following Eq. (6):

$$n_{Si–O–M} = n_{total} \cdot X_O \cdot f_{Si–O–M}, \quad \text{..... (6)}$$

where $n_{total}$, $X_O$, and $f_{Si–O–M}$ are atomic number density of the glass, oxygen atomic fraction, and the fraction of oxygen atoms bonded with silicon and metallic cations, respectively. The present study derived the $n_{total}$ ($=N_A\rho/Y$)[39] from the measured density ($\rho$) and the Avogadro's number ($=6.02\times10^{23}$) where Y is the average molecular weight of the samples. $f_{Si–O–M}$ was derived using Eq. (7):[40,41]

$$f_{Si–O–M} = \frac{2X_O - 4X_{Si}}{X_O}, \quad \text{..... (7)}$$

where $X_{Si}$ denotes the atomic fraction of Si. Previous studies have validated that $f_{Si–O–M}$ obtained using Eq. (7) agree well with the experimental values obtained using spectroscopic techniques for the silicate glasses.[42–44] The phonon MFP of the glasses was derived using Eq. (3), as listed in Table 2. The phonon MFPs of the silicate glasses are plotted against $n_{Si–O–M}$ in **Fig. 4**. The phonon MFP for the pure silica glass was close to 0.6 nm, which is similar to the interatomic distance from a silicon atom to its second neighbor silicon atom (Si–O–Si–O–Si),[27] as drawn in Fig. 1. The phonon MFP decreased with the addition of metallic oxides. These data indicate that phonon scattering is more likely to occur near metallic cations. Since the phonon MFP is similar for alkali or alkaline-earth cations at a comparable $n_{Si–O–M}$ (see Fig. 4), herein the phonon MFP evolution was fitted against the $n_{Si–O–M}$ for the alkali and alkaline-earth silicate systems by the single nonlinear regression curve, which is expressed by the following Eq. (8):

$$l = a + \frac{1}{b\left(n_{Si–O–M} + c\right)}. \quad \text{..... (8)}$$

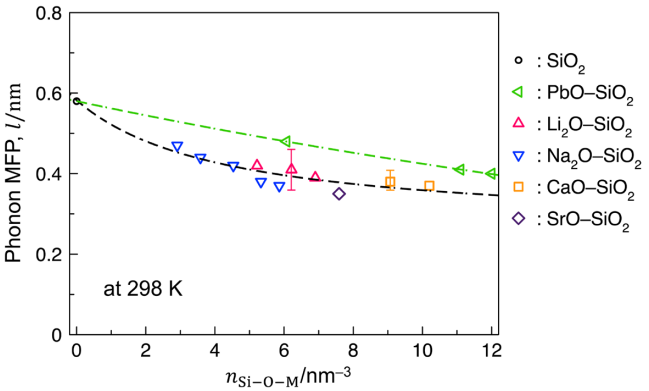


**Fig. 4.** Evolution of the phonon MFP with $n_{Si–O–M}$ for the glass samples. The possible error range of the phonon MFP was evaluated based on the scatter in the measured values of the thermal diffusivity and shown as the error bars. For plots without an error bar, the error range is smaller than the size of the plots. The green and black dashed lines represent the fitting curves by Eq. (8) for lead silicate and alkali or alkaline-earth silicate systems, respectively. (Online version in color.)

The physical meaning of the fitting parameters ($a$ and $c$) in Eq. (8) remains unclear whereas the parameter $b$ ($=0.73$), which reflects the steepness of the variation in the phonon MFP with increasing the $n_{Si–O–M}$, should relate to the probability of phonon scattering near metallic cations. Notably, the phonon MFP values of lead silicate glasses are higher than those of alkali or alkaline-earth silicate glasses with similar $n_{Si–O–M}$ values. The evolution of the phonon MFP against $n_{Si–O–M}$ for the lead silicate systems are also well reproduced by the Eq. (8) with the lower $b$ value (0.02), which indicates that the probability of the phonon scattering is lower for the lead silicate system than those for the alkali and alkaline-earth silicate systems. The following discussion considers the origin of the composition-induced variation in the phonon MFP from the viewpoint of the bonding character near the metallic cations.

## 5. Discussion

In silicate glasses, metallic cations are surrounded by several oxygen atoms and form polyhedral species ($MO_N$), which link with $SiO_4$ tetrahedra with different bond

strengths and connectivities (*e.g.*, corner- and edge-sharing linkages). The incoherence of the vibration mode near the Si–O–M bond should change depending on its bond character: "bond strengths" and "connectivity." To evaluate the bond strength, Pauling[45] proposed the concept of electrostatic valence bond strength, which is described by the cationic valence divided by its coordination number ($Z/N$).[46,47] The connectivity shows different aspects of the bond character, which, however, should not be completely independent of the $Z/N$ of the metallic cations. Generally, two types of connectivity (linkages) are found in silicate glasses: "corner-" and "edge-sharing" linkages, as depicted in **Fig. 5**. When a metallic cation ($M^{n+}$) has a high $Z/N$, the $MO_N$ polyhedral species prefer to bond with $SiO_4$ by corner-sharing linkages to retain a long Si–M distance and weaken the cation-cation repulsion.[45] Meanwhile, a low $Z/N$ ratio of an M cation allows for a shorter Si–M distance and partly for the formation of an edge-sharing linkage between $SiO_4$ and $MO_N$. The present study estimated the $Z/N$ ratios for selected metallic cations: $Si^{4+}$, $Li^+$, $Na^+$, $Ca^{2+}$, $Sr^{2+}$, and $Pb^{2+}$. **Table 3** shows the estimated $Z/N$ values for these

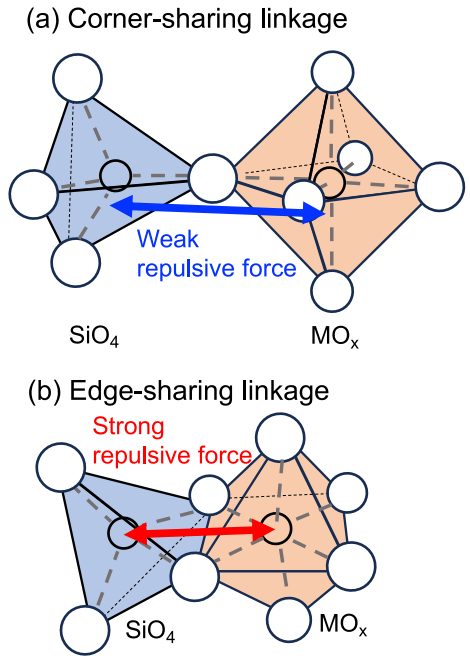


**Fig. 5.** Schematic illustrations of (a) corner-sharing and (b) edge-sharing $SiO_4$–$MO_N$ linkages. (Online version in color.)

**Table 3.** Formal cationic valence ($Z$) and reported coordination number ($N$)[48–51] for the chosen cationic species. The fraction of the edge-sharing linkage was categorized into three categories depending on our assumption based on the results of structural characterization: Non, Low, and High.

| | $Si^{4+}$ | $Pb^{2+}$ | $Ca^{2+}$ | $Sr^{2+}$ | $Li^+$ | $Na^+$ |
|---|---|---|---|---|---|---|
| $Z$ | 4 | 2 | 2 | 2 | 1 | 1 |
| $N$ | 4 | 3.5* | 6 | 7.5* | 4 | 6 |
| $Z/N$ | 1 | 0.57 | 0.33 | 0.26 | 0.25 | 0.17 |
| Fraction of edge-sharing | Non | Low | High | High | High | High |

*Intermediate values in the range of the reported coordination numbers[49,51]

cations, based on the reported coordination numbers ($N$) for the cations: Si,[48] Pb,[49] Ca,[50] Sr,[51] Li,[48] and Na.[48] $Si^{4+}$ has a high $Z/N$ of 1 whereas the $Z/N$ of alkali and alkaline-earth cations was lower than that of silicon cation and in the range of 0.17–0.33. The calculated $Z/N$ indicates that the bond strength near the alkali and alkaline-earth cations differs depending on the type of cation; however, the phonon MFPs of the alkali and alkaline-earth silicate glasses do not change with the type of metallic cations when their $n_{Si–O–M}$ values are comparable, as shown in Fig. 4. This indicates that the effect of the bond strength near the metallic cations on the phonon MFP was small for the chosen alkali and alkaline-earth silicate glasses.

The remaining aspect of the bond character is the connectivity of the polyhedral linkages. Since it has been reported the repulsive force between two cations in the edge-sharing linkage affects the thermal vibration mode in oxide crystalline materials,[52] the fraction of the minor edge-sharing linkage in silicate glasses should affect the phonon MFP, whereas the corner-sharing linkage is the main type of the connection in oxide glasses.[53] Based on the calculated $Z/N$, the polyhedral unit with $Pb^{2+}$ (*e.g.*, $PbO_4$) tended to have a lower fraction of edge-sharing linkages than the polyhedral species of alkali and alkaline-earth cations. Some authors have clarified the atomic arrangement of the $22.7Na_2O$–$77.3SiO_2$ (mol%),[54] $33PbO$–$67SiO_2$ (mol%),[55] and $50PbO$–$50SiO_2$ (mol%)[55] glasses using X-ray and neutron scattering with the aid of computer simulation based on reverse Monte Carlo (RMC) modeling. The present study recharacterized the RMC-modeled atomic arrangement and derived the fraction of edge-sharing connections for the $SiO_4$–$MO_N$ linkage from the partial pair distribution functions for Pb–Si and Na–Si. The obtained fraction of edge-sharing linkages was 9% for the $SiO_4$–$NaO_N$ in the $22.7Na_2O$–$77.3SiO_2$ (mol%) glass, whereas those of the $SiO_4$–$PbO_N$ were 4% and 2% for the $33PbO$–$67SiO_2$ (mol%) and $50PbO$–$50SiO_2$ (mol%) glasses, respectively. Although we did not characterize the fraction of edge-sharing linkages for the $SiO_4$–$MO_N$ for all the glass systems, Toyoda *et al.*[56] have recently reported that the fraction of edge-sharing linkages for the $SiO_4$–$LiO_N$ in a lithium silicate-based multicomponent glass was close to 10%, which is relatively similar to the fraction in the sodium silicate glass. Assuming that the fractions of edge-sharing linkage in the lithium, calcium, and strontium silicate systems are similar to that of the sodium silicate glass, the polyhedral unit with $Pb^{2+}$ tended to have a lower fraction of edge-sharing linkages than the polyhedral species of alkali and alkaline-earth cations, as estimated from $Z/N$. The current MFP data allow us to hypothesize that the repulsive force between Si and metallic cations in the edge-sharing linkage generates an incoherent vibration mode, which tends to scatter phonons in the silicate glass structure.

Metallic cations in silicate glasses and melts are categorized into framework and non-framework cations. The former have a high $Z/N$ ratio and constructs a silicate network structure by forming a corner-sharing linkage between $SiO_4$ and $MO_N$, as proposed by Zachariasen.[53] The latter, which generally have a low $Z/N$, tends to break the silicate network structure. The structural roles of metallic cations in silicate glass have been extensively studied through structural characterization[57,58] and physical prop-

erty measurements.[59,60] Silicon cations were determined to act as framework cations, whereas alkali and alkaline-earth cations act as nonframework cations.[61,62] In contrast, the structural role of lead cations in silicate glasses remains inconclusive. Kohara *et al.*[55] reported that $Pb^{2+}$ cations partly act as framework cations (network formers) based on the extraordinarily large amount of free volume (voids) in lead silicate glass, which cannot be found in conventional binary silicate glasses containing nonframework cations (*e.g.*, alkali silicate glasses). Kacem *et al.*[63] reported that lead cations act as nonframework cations (network modifiers) based on the glass-transition temperature ($T_g$) data for binary silicate glasses, and the larger decrease in the $T_g$ of silica glass with the addition of lead oxide than that with the addition of a comparable calcium oxide content. Our finding contradicts the compositional dependence of $T_g$, where lead silicate glasses have higher phonon MFPs than alkali and alkaline-earth silicate glasses at comparable $n_{Si–O–M}$ values. In particular, these results indicate that phonons propagate through Si–O–Pb bonds with a higher probability than through Si–O–R bonds, where R represents an alkaline or alkaline-earth atom. This tendency indicates that lead cations partly act as framework cations from the viewpoint of phonon propagation. The structural role estimated by the phonon MFP is consistent with the conclusion from the free-volume analysis but contradicts the interpretation from the $T_g$ data. These different conclusions could be ascribed to the differences in the dominant parameters of $T_g$ and phonon MFP. Assuming that $T_g$ is the temperature at which the structure of glass starts to relax via viscous flow, $T_g$ should be influenced by the mobility of the oxygen atoms near the metallic cations.[64,65] As the oxygen atoms between silicon and lead atoms (Si–O–Pb) have a higher mobility than those between two silicon atoms (Si–O–Si), Si–O–Pb bonds should behave in the breakage of the silicate network structure from the viewpoint of viscous flow ($T_g$). In contrast, phonon MFP was dominated by the connectivity of the polyhedral species. The corner-sharing Si–O–Pb linkage acts as a connected part of the network structure for phonon propagation. Although the compositional dependence of $T_g$ and phonon MFP obtained opposite conclusions on the structural role of lead cations, the structural role of lead cations is categorized differently depending on the types of properties. Zachariasen[53] proposed empirical rules to distinguish oxide components based on the glass-forming abilities. According to these rules, oxygen polyhedra of metallic cations must share corners rather than edges or faces to form glass. Interestingly, the classification of the structural role of metallic cations by phonon MFP conforms to Zachariasen's rules[53] for the polyhedral connectivity in the chosen compositions. Further studies on the phonon MFP of oxide glasses containing other types of framework and nonframework cations with detailed structural information are required to fully understand the origin of the composition-induced variation in phonon MFP.

## 6. Conclusion

This study investigated the variation in the phonon MFP of binary silicate glasses at 298 K by adding $M_{2/n}O$ ($M^{n+}$: $Li^+$, $Na^+$, $Ca^{2+}$, $Sr^{2+}$, or $Pb^{2+}$). The MFP decreased with an increase in $SiO_4$–$MO_N$ linkages in the glasses. The MFPs of alkali and alkaline earth silicate glasses are similar when the number densities of oxygen atoms between the silicon and metallic cations ($n_{Si–O–M}$) are comparable. This indicates that the MFP does not strongly depend on the type of alkali or alkaline earth cation. However, the MFP of lead silicate glass was higher than those of the alkali and alkaline-earth silicate systems when $n_{Si–O–M}$ is comparable. This tendency can be explained by the differences in the fraction of edge-sharing linkages where phonons tend to be scattered. Our phonon MFP data indicate that lead cations partially act as framework cations from the viewpoint of phonon propagation.

## Conflict of Interest

The authors declare that there is no conflict of interest.

## Acknowledgments

This work was done as an activity of the ISIJ Research group I "Improvement of measurement accuracy in thermal conductivity of molten oxides (2022–2024)," which was financially supported by the Iron and Steel Institute of Japan (ISIJ). We appreciate the members of the research group for their fruitful discussion. This work was partially supported by JSPS KAKENHI (JP24K01153 and JP21H01854), the cooperative research program of "Network Joint Research Center for Materials and Devices (MEXT), and the research grant from the Nippon Sheet Glass Foundation for Materials Science and Engineering. We thank Mr. Shigeru Suzuki (Japan Steel Works, Ltd.) for his contribution to the chemical analysis of the samples. The authors are grateful to Mr. Yoshihiro Nakamura (Tohoku University) for carefully polishing the glass sample surfaces. We appreciate the constructive comments of the anonymous reviewer and editor for improving our manuscript.

## REFERENCES

1) J. Yang, Z. Wang and I. Sohn: *Acta Mater.*, **234** (2022), 118014. https://doi.org/10.1016/j.actamat.2022.118014
2) Y. Dong, Z. Jiang, Y. Cao, D. Hou, L. Liang and J. Duan: *ISIJ Int.*, **55** (2015), 904. https://doi.org/10.2355/isijinternational.55.904
3) L. Pilon, F. Janos and R. Kitamura: *J. Am. Ceram. Soc.*, **97** (2014), 442. https://doi.org/10.1111/jace.12768
4) T. Kanazawa, S. Hiraki, M. Kawamoto, K. Nakai, K. Hanazaki and T. Murakami: *Tetsu-to-Hagané*, **83** (1997), 701 (in Japanese). https://doi.org/10.2355/tetsutohagane1955.83.11_701
5) M. Hanao and M. Kawamoto: *ISIJ Int.*, **48** (2008), 1210. https://doi.org/10.2355/isijinternational.48.1210
6) S. Takahashi, R. Endo, T. Watanabe, M. Hayashi and M. Susa: *ISIJ Int.*, **58** (2018), 905. https://doi.org/10.2355/isijinternational.ISIJINT-2017-661
7) Y. Kang, J. Lee and K. Morita: *ISIJ Int.*, **54** (2014), 2008. https://doi.org/10.2355/isijinternational.54.2008
8) K. C. Mills and C.-Å. Däcker: The Casting Powders Book, Springer International Publishing, Cham, (2017), 177.
9) L. Liu, X. Han, D. Zhang, M. Li and Y. Wang: *ISIJ Int.*, **63** (2023), 1697. https://doi.org/10.2355/isijinternational.ISIJINT-2022-548
10) D. Chebykin, I. Saenko, H.-P. Heller, R. Endo and O. Volkova: *J. Non-Cryst. Solids*, **622** (2023), 122644. https://doi.org/10.1016/j.jnoncrysol.2023.122644
11) M. Susa, N. Tsuchida, R. Endo and Y. Kobayashi: *Tetsu-to-Hagané*, **95** (2009), 289 (in Japanese). https://doi.org/10.2355/tetsutohagane.95.289
12) Z. Zhang, D.-B. Zhang, K. Onga, A. Hasegawa, K. Ohta, K. Hirose and R. M. Wentzcovitch: *Phys. Rev. B*, **104** (2021), 184101. https://doi.org/10.1103/PhysRevB.104.184101
13) A. K. Varshneya and J. C. Mauro: Fundamentals of Inorganic Glasses (3rd ed.), ed. by A. K. Varshneya and J. C. Mauro, Elsevier, (2019), 283.
14) S. S. Sørensen, E. J. Pedersen, F. K. Paulsen, I. H. Adamsen, J. L. Laursen, S. Christensen, H. Johra, L. R. Jensen and M. M. Smedskjaer:

*Appl. Phys. Lett.*, **117** (2020), 031901. https://doi.org/10.1063/5.0013400
15) S. Sukenaga, T. Endo, T. Nishi, H. Yamada, K. Ohara, T. Wakihara, K. Inoue, S. Kawanishi, H. Ohta and H. Shibata: *Front. Mater.*, **8** (2021), 753746. https://doi.org/10.3389/fmats.2021.753746
16) R. Peierls: *Annalen der Physik*, **395** (1929), 1055. https://doi.org/10.1002/andp.19293950803
17) J. F. Stebbins, I. S. E. Carmichael and L. K. Moret: *Contrib. Mineral. Petrol.*, **86** (1984), 131. https://doi.org/10.1007/BF00381840
18) P. Richet: *Chem. Geol.*, **62** (1987), 111. https://doi.org/10.1016/0009-2541(87)90062-3
19) T. Sugawara, Y. Hamano, S. Yoshida and J. Matsuoka: *J. Ceram. Soc. Jpn.*, **121** (2013), 972. https://doi.org/10.2109/jcersj2.121.972
20) Y. Shi, A. Tandia, B. Deng, S. R. Elliott and M. Bauchy: *Acta Mater.*, **195** (2020), 252. https://doi.org/10.1016/j.actamat.2020.05.047
21) C. Kittel: *Phys. Rev.*, **75** (1949), 972. https://doi.org/10.1103/PhysRev.75.972
22) Y. Hiroshima, Y. Hamamoto, S. Yoshida and J. Matsuoka: *J. Non-Cryst. Solids*, **354** (2008), 341. https://doi.org/10.1016/j.jnoncrysol.2007.08.082
23) S. Inaba, S. Oda and K. Morinaga: *J. Japan Inst. Met.*, **65** (2001), 680. https://doi.org/10.2320/jinstmet1952.65.8_680
24) F. Li, M. Susa and K. Nagata: *J. Japan Inst. Met.*, **55** (1991), 194. https://doi.org/10.2320/jinstmet1952.55.2_194
25) K. Nagata, K. Ohira, H. Yamada and K. S. Goto: *Metall. Trans. B*, **18** (1987), 549. https://doi.org/10.1007/BF02654267
26) Y. Kim and K. Morita: *J. Am. Ceram. Soc.*, **98** (2015), 1588. https://doi.org/10.1111/jace.13490
27) Y. Waseda and J. M. Toguri: *Metall. Trans. B*, **9** (1978), 595. https://doi.org/10.1007/BF03257207
28) A. M. Hofmeister: Measurements, Mechanisms, and Models of Heat Transport, ed. by A. M. Hofmeister, Elsevier, (2019), 75.
29) H. Ohno, T. Nagasaki, N. Igawa and H. Kawamura: *J. Nucl. Mater.*, **179–181** (1991), 473. https://doi.org/10.1016/0022-3115(91)90127-S
30) S. Sukenaga, H. Unozawa, Y. Chiba, M. Tashiro, S. Kawanishi and H. Shibata: *J. Am. Ceram. Soc.*, **106** (2023), 293. https://doi.org/10.1111/jace.18760
31) O. V. Mazurin, M. V. Streltsina and T. P. Shvaiko-Shvaikovskaya: Hand Book of Glass Data, Physical Sciences Data, Vol. 15, Elsevier, (1983), 186.
32) O. V. Mazurin, M. V. Streltsina and T. P. Shvaiko-Shvaikovskaya: Hand Book of Glass Data, Physical Sciences Data, Vol. 15, Elsevier, (1983), 463.
33) M. Li, M. Akoshima and N. Yamada: *Int. J. Therm. Sci.*, **165** (2021), 106955. https://doi.org/10.1016/j.ijthermalsci.2021.106955
34) H. Shibata, H. Ohta, A. Suzuki and Y. Waseda: *Mater. Trans., JIM*, **41** (2000), 1616. https://doi.org/10.2320/matertrans1989.41.1616
35) J. A. Cape and G. W. Lehman: *J. Appl. Phys.*, **34** (1963), 1909. https://doi.org/10.1063/1.1729711
36) T. Rouxel: *J. Am. Ceram. Soc.*, **90** (2007), 3019. https://doi.org/10.1111/j.1551-2916.2007.01945.x
37) J. P. Guin and Y. Gueguen: Mechnical Properties of Glass, Springer Handbook of Glass, ed. by J. D. Musgraves *et al.*, Springer, (2019), 227. https://doi.org/10.1007/978-3-319-93728-1_7
38) S. Chapman and T. G. Cowling: The Mathematical Theory of Non-uniform Gases, 3rd ed., Campbidge University Press, (1990), 88.
39) S. Sukenaga and H. Shibata: High-Temperature Characterization of Glasses and Melts, Encyclopedia of Materials: Techinical Ceramics and Glasses, Vol. 1, (2021), 689. https://doi.org/10.1016/B978-0-12-818542-1.00024-2
40) B. Mysen and P. Richet: Silicate Glasses and Melts (2nd ed.), ed. by B. Mysen and P. Richet, Elsevier, (2019), 109.
41) S. Sukenaga, T. Higo, H. Shibata, N. Saito and K. Nakashima: *ISIJ Int.*, **55** (2015), 1299. https://doi.org/10.2355/isijinternational.55.1299
42) J. F. Stebbins, E. V. Dubinsky, K. Kanehashi and K. E. Kelsey: *Geochim. Cosmochim. Acta*, **72** (2008), 910. https://doi.org/10.1016/j.gca.2007.11.018
43) S. Sukenaga, P. Florian, K. Kanehashi, H. Shibata, N. Saito, K. Nakashima and D. Massiot: *J. Phys. Chem. Lett.*, **8** (2017), 2274. https://doi.org/10.1021/acs.jpclett.7b00465
44) S. K. Lee and E. J. Kim: *J. Phys. Chem. C*, **119** (2015), 748. https://doi.org/10.1021/jp509780f
45) L. Pauling: *J. Am. Chem. Soc.*, **51** (1929), 1010. https://doi.org/10.1021/ja01379a006
46) I. D. Brown: The Chemical Bond in Inorganic Chemistry, Oxford University Press, (2016), 27.
47) S. Sukenaga, K. Kanehashi, H. Yamada, K. Ohara, T. Wakihara and H. Shibata: *ISIJ Int.*, **63** (2023), 1263. https://doi.org/10.2355/isijinternational.ISIJINT-2022-398
48) Y. Waseda and H. Suito: *Trans. ISIJ*, **17** (1977), 82. https://doi.org/10.2355/isijinternational1966.17.82
49) O. L. G. Alderman, A. C. Hannon, D. Holland, R. Dupree, G. Lehr, A. Vitale and S. Feller: *J. Am. Ceram. Soc.*, **105** (2022), 938. https://doi.org/10.1111/jace.18125
50) Y. Waseda and J. M. Toguri: *Metall. Trans. B*, **8** (1977), 563. https://doi.org/10.1007/BF02669331
51) T. Charpentier, K. Okhotnikov, A. N. Novikov, L. Hennet, H. E. Fischer, D. R. Neuville and P. Florian: *J. Phys. Chem. B*, **122** (2018), 9567. https://doi.org/10.1021/acs.jpcb.8b05721
52) A. Nakatsuka, K. Sugiyama, A. Yoneda, K. Fujiwara and A. Yoshiasa: *Acta Cryst. E*, **71** (2015), 1109. https://doi.org/10.1107/S2056989015015649
53) W. H. Zachariasen: *J. Am. Chem. Soc.*, **54** (1932), 3841. https://doi.org/10.1021/ja01349a006
54) Y. Onodera, Y. Takimoto, H. Hijiya, T. Taniguchi, S. Urata, S. Inaba, S. Fujita, I. Obayashi, Y. Hiraoka and S. Kohara: *NPG Asia Mater.*, **11** (2019), 75. https://doi.org/10.1038/s41427-019-0180-4
55) S. Kohara, H. Ohno, M. Takata, T. Usuki, H. Morita, K. Suzuya, J. Akola and L. Pusztai: *Phys. Rev. B*, **82** (2010), 134209. https://doi.org/10.1103/PhysRevB.82.134209
56) R. Toyoda, K. Usui, T. Hirota, K. Kimura, Y. Onodera, M. R. Cicconi, R. Belli, M. Brehl, J. Lubauer, U. Lohbauer, H. Tajiri, K. Ikeda, T. Hayakawa, D. de Ligny, S. Kohara and K. Hayashi: *J. Non-Cryst. Solids*, **616** (2023), 122472. https://doi.org/10.1016/j.jnoncrysol.2023.122472
57) F. Fayon, C. Landron, K. Sakurai, C. Bessada and D. Massiot: *J. Non-Cryst. Solids*, **243** (1999), 39. https://doi.org/10.1016/S0022-3093(98)00809-6
58) B. Mysen: *ISIJ Int.*, **61** (2021), 2866. https://doi.org/10.2355/isijinternational.ISIJINT-2021-100
59) J. O. Bockris and G. W. Mellors: *J. Phys. Chem.*, **60** (1956), 1321. https://doi.org/10.1021/j150543a040
60) N. W. Nesbitt and M. E. Fleet: *Geochim. Cosmochim. Acta*, **45** (1981), 235. https://doi.org/10.1016/0016-7037(81)90168-X
61) C. Le Losq, M. R. Cicconi, G. N. Greaves and D. R. Neuville: Silicate Glasses, Springer Handbok of Glass, ed. by J. D. Musgraves *et al.*, Springer, (2019), 441. https://doi.org/10.1007/978-3-319-93728-1_13
62) G. S. Henderson: *Canad. Mineral.*, **43** (2005), 1921. https://doi.org/10.2113/gscanmin.43.6.1921
63) I. B. Kacem, L. Gautron, D. Coillot and D. R. Neuville: *Chem. Geol.*, **461** (2017), 104. https://doi.org/10.1016/j.chemgeo.2017.03.030
64) D. B. Dingwell and S. L. Webb: *Phys. Chem. Mineral.*, **16** (1989), 508. https://doi.org/10.1007/BF00197020
65) S. Sukenaga, Y. Gueguen, F. Cerarie, T. Roxel, M. Tashiro, S. Yoshida, N. Saito, K. Nakashima and H. Shibata: *J. Am. Ceram. Soc.*, **107** (2024), 3822. https://doi.org/10.1111/jace.19722